Title
Mutant Evolution in Spatially Structured and Fragmented Expanding Populations.

Permalink
https://escholarship.org/uc/item/2t6702h9

Journal
Genetics, 216(1)

ISSN
0016-6731

Authors
Wodarz, Dominik
Komarova, Natalia L

Publication Date
2020-09-01

DOI
10.1534/genetics.120.303422

Peer reviewed

Mutant Evolution in Spatially Structured and Fragmented Expanding Populations

Dominik Wodarz*,†,1 and Natalia L. Komarova†,1

*Department of Population Health and Disease Prevention, Program in Public Health, Susan and Henry Samueli College of Health Sciences and †Department of Mathematics, University of California Irvine, California 92697

ORCID IDs: 0000-0002-8017-3707 (D.W.); 0000-0003-4876-0343 (N.L.K.)

ABSTRACT Mutant evolution in spatially structured systems is important for a range of biological systems, but aspects of it still require further elucidation. Adding to previous work, we provide a simple derivation of growth laws that characterize the number of mutants of different relative fitness in expanding populations in spatial models of different dimensionalities. These laws are universal and independent of "microscopic" modeling details. We further study the accumulation of mutants and find that, with advantageous and neutral mutants, more of them are present in spatially structured, compared to well-mixed colonies of the same size. The behavior of disadvantageous mutants is subtle: if they are disadvantageous through a reduction in division rates, the result is the same, and it is the opposite if the disadvantage is due to a death rate increase. Finally, we show that in all cases, the same results are observed in fragmented, nonspatial patch models. This suggests that the patterns observed are the consequence of population fragmentation, and not spatial restrictions *per se*. We provide an intuitive explanation for the complex dependence of disadvantageous mutant evolution on spatial restriction, which relies on desynchronized dynamics in different locations/patches, and plays out differently depending on whether the disadvantage is due to a lower division rate or a higher death rate. Implications for specific biological systems, such as the evolution of drug-resistant cell mutants in cancer or bacterial biofilms, are discussed.

KEYWORDS evolutionary dynamics; fragmented populations; mathematical models; spatial dynamics

THE dynamics of mutant creation and invasion are relatively well understood under a variety of conditions and assumptions, mostly assuming perfect mixing of individuals. In the context of constant populations, the fixation probability of mutants, as well as fixation times, have been thoroughly defined under various assumptions in the population genetics literature (Kimura 1962; Patwa and Wahl 2008). The emergence of mutants in exponentially growing bacterial populations is also well studied, based on the famous Luria-Delbruck experiments (Luria and Delbruck 1943) and the resulting rich theoretical framework (Zheng 1999; Kepler and Oprea 2001; Dewanji *et al.* 2005; Komarova *et al.* 2007). This has been instrumental for understanding the principles according to which antibiotic-resistant microbes emerge (Johnson and

Levin 2013), and has also been applied to studying the emergence of drug resistance in some cancers (Coldman and Goldie 1983; Goldie and Coldman 1998; Komarova and Wodarz 2005). The majority of tumors, however, are characterized by the growth of two-dimensional (2D) and three-dimensional (3D) spatial structures, and so is the growth of bacteria in biofilms. Recent experimental and theoretical work (Fusco *et al.* 2016) has extended our understanding of mutant emergence in such spatially structured, expanding populations. An excess of mutational jackpot events was observed in spatial compared to well-mixed systems. Such events result from mutations arising at the surface of expanding, spatially structured populations, surfing at the edge of range expansions, and appearing as mutant "sectors" or "slices." These jackpot events can occur relatively late in the expansion process, which is in contrast to well-mixed systems in which mutational jackpot events can only occur early on in the population growth process (Fusco *et al.* 2016). Hence, overall, the average number of mutants when the total population reaches a given threshold size is significantly larger in spatial compared to nonspatial settings (Fusco *et al.* 2016).

This work was done under the assumption that cells do not die, and theory and computations were mostly developed in the context of neutral mutants. A number of other papers studied the spread of mutants in spatial and fragmented settings. A study by Gralka and Hallatschek (2019) considered the spread of advantageous mutants focusing on the role of habitat fragmentation. In Gralka *et al.* (2016), several scaling relationships for individual mutant clones were derived, including advantageous mutants, in the context of expanding 2D colonies, both "flat" and radial. Spatial dynamics of disadvantageous mutants were studied by Otwinowski and Krug (2014), focusing on Write–Fischer dynamics in constant populations, and by Lavrentovich *et al.* (2016), who looked at the mutational meltdown. The dynamics of advantageous mutants in a 3D patch model was studied by Waclaw *et al.* (2015) in the context of tumors.

Here, we build on the existing work and investigate the dynamics of mutant emergence and growth in spatially structured cell populations assuming varying death rates, different mutant fitness, different dimensionalities of space, and different spatial modeling approaches. One of the two main messages of this paper is to report interesting dynamics observed for disadvantageous mutants, which could apply for example to drug-resistant mutants that emerge before the onset of therapy. If the disadvantage is caused by a larger death rate of the mutant cells, then we find that, in contrast to other scenarios, the number of mutants at a given size can be larger in a well-mixed compared to the spatial system. If, on the other hand, the fitness disadvantage arises because of a slower replication rate, then more mutants are found in the spatial compared to the nonspatial system, similar to the results obtained for neutral or advantageous mutants.

The second message is that surprisingly similar results are obtained in explicitly spatial models and in patch models, where local within-patch dynamics are governed by perfect mixing, but individuals migrate to other patches. Interestingly, the results do not depend on the assumption that patches are spatially arranged, with migration of individuals to nearest neighboring patches. The same outcomes are observed if migration can occur to any randomly chosen patch in the system. Therefore, the properties of mutant growth in the spatial agent-based model might not be the direct consequence of spatial dynamics, but the consequence of population fragmentation.

In addition, in this paper we provide a simple and straightforward derivation of scaling growth laws that govern cell expansion in spatially constrained models. The so-called "surface growth" law of homogeneous cell colonies in space has previously been described in experiments (Freyer and Sutherland 1985; Brú *et al.* 1998; Günther *et al.* 2007) and in the modeling literature (Brú *et al.* 2003; Block *et al.* 2007; Komarova and Wodarz 2010; Rodriguez-Brenes *et al.* 2013; Talkington and Durrett 2015; Murphy *et al.* 2016). Here, we study the laws of mutant generation, spread, and competition with wild-type individuals, in the context of spatially restricted colony expansion. We derive formulas that relate the expected number of disadvantageous, neutral, and advantageous mutants to the total population size in different spatial dimensions. While some of these laws have been derived previously [such as the growth laws of neutral mutants (Fusco *et al.* 2016)], others are novel or confirm previous numerical observations [see the conjecture of paper (f) on advantageous mutant growth in 2D expansion].

Materials and Methods

Two-dimensional agent-based model

We used a two-dimensional, agent-based model, where a two-dimensional square grid is considered. A spot on the grid can be empty or can contain a cell, which is either wild-type or mutant. At each time step, the grid is randomly sampled N times, where N is the total number of cells currently in the system. If the sampled cell is wild type, the cell attempts division (described below) with a probability L_w or dies with a probability D_w. When reproduction is attempted, a target spot is chosen randomly from the nearest neighbors of the cell (eight neighbors, *i.e.*, the Moore neighborhood, was used unless otherwise noted). If that spot is empty, the offspring cell is placed there. If it is already filled, the division event is aborted. The offspring cell is assigned wild type with probability $1-u$ and it is a mutant with probability u. If the sampled spot contains a mutant cell, the same processes occur. Attempted division occurs with a probability L_m, and the cell dies with a probability D_m. The offspring of a mutant cell is always a mutant in the absence of back mutation. In a different version of the model, a mutant's offspring can be of wild-type with probability u. Initial and boundary conditions are determined by the specific geometric setting investigated. For 2D spatial simulations, an $n{\times}n$ square domain is considered. At the boundaries of the domain, a spot is assumed to have fewer neighbors, *i.e.*, more division events will fail. The simulations start with a single wild-type cell, placed into the center of the grid. Simulations always stop before the boundary of the grid is reached. For 1D cylinder simulations, we use an $n{\times}w$ rectangular domain of width w. We start with an array of w wild-type cells at the left boundary of the domain, and impose periodic boundary conditions in the transversal direction. In each simulation, the cell population is allowed to grow to a size M, and the number of mutant cells at this size is recorded. Such simulations are performed repeatedly, and the average number of mutants is calculated. Simulation runs, in which the total cell population goes extinct due to stochastic effects, are ignored.

Analysis of 2D spatial stochastic models is presented in Section 3 of the Supplemental material. Growth laws for different geometries are derived in Section 4 of the Supplement.

Modeling exponential growth

To compare the spatial dynamics to a well-mixed system, we considered a simple stochastic simulation of exponential

growth. Denoting the number of wild-type cells with x_w and the number of mutant cells with x_m, one of the cell types is chosen with a probability given by their proportion in the whole cell population. Wild types can divide with a probability L_w and can die with a probability D_w. Mutants can divide with a probability l_m and die with a probability d_m. Mutations of wild-type cells happen with probability u. As in the spatial system, the average number of mutants at population size M was determined.

A patch (island/metapopulation) model

We also considered an alternative modeling approach to capture mutant dynamics in spatially structured populations. Instead of tracking the spatial location of individual cells, we analyze a model that consists of a 2D grid of nxn patches or demes. Deme models to approximate spatial dynamics have been explored before (Waclaw *et al.* 2015), and our approach is conceptually related. Within each patch, local dynamics occur where cells are assumed to mix perfectly. At each time step, cells are allowed to migrate to a different patch with a given rate. In each local patch, Gillespie simulations (Gillespie 1977) of the following ordinary differential equation model were run:

$$\frac{dx_i}{dt} = l_w x_i (1-u)\left(1 - \frac{x_i + y_i}{k}\right) - d_w x_i - m x_i + \frac{m}{8} \sum_{neighbors, j} x_j$$

$$\frac{dy_i}{dt} = u l_w x_i \left(1 - \frac{x_i + y_i}{k}\right) + l_m y \left(1 - \frac{x_i + y_i}{k}\right)$$
$$- d_m y_i - m y_i + \frac{m}{8} \sum_{neighbors, j} y_j$$

Wild-type cells are denoted by x_i, and mutant cells by y_i, where the subscript i enumerates the spatial locations in a 2D array. Wild-type cells divide with a density-dependent rate $l_w [1-(x+y)/k]$, die with a rate d_w, and migrate out of the patch with a rate m. Migration is assumed to occur to one of the eight neighboring patches, chosen randomly. During replication of the wild-type cells, a mutant cell can be generated with a probability u. Mutant cells divide with a density-dependent rate $l_m [1-(x+y)/k]$, die with a rate d_m, and migrate with a rate m.

In an alternative (fragmentation) model, instead of migrating with rate $m/8$ per patch to one of the eight neighboring patches, cells migrate with probability $m/(n-1)$ per patch to any other patch regardless of its location. This holds for cells in all the patches in the system, thus removing a spatial component from the migration process. Otherwise, the equations are identical to the ones above.

Simulations were started with a single wild-type cell in the middle patch. The simulations were run until the total cell population size, summed over all patches, reached size M. At this point, the number of mutants summed over all patches was recorded. This was done repeatedly, and the average number of mutants at size M was determined. Instances of the simulation that resulted in population extinction across all patches were ignored.

For comparison, Gillespie simulations were performed in a nonfragmented, well-mixed system described by the following equations:

$$\dot{x} = l_w x (1-u)\left(1 - \frac{x+y}{n^2 k}\right) - d_w x,$$
$$\dot{y} = u l_w x \left(1 - \frac{x+y}{n^2 k}\right) + l_m y \left(1 - \frac{x+y}{n^2 k}\right) - d_m y$$

The carrying capacity of the nonfragmented system is taken n^2 times the carrying capacity of the individual patches (n^2 is the total number of patches). The average number of mutants at population size M was determined in the same way as in the patch model.

Deterministic [ordinary differential equations (ODE)] versions of these models are presented in Section 2 of the Supplemental material.

Data availability

This paper uses mathematical models and does not have new data. Supplemental material available at figshare: https://doi.org/10.25386/genetics.12645377. The authors state that all data necessary for confirming the conclusions presented in the article are represented fully within the article.

Results

Generation and spread of mutants in spatial and nonspatial models

We used a 2D agent-based model and a patch model (see *Materials and Methods*) to explore the spread of mutants in spatial and nonspatial growth processes. Denote by L_w and L_m, the division rates of wild type and mutant cells, and by D_w and D_m their respective death rates. Below we report the results for neutral, disadvantageous, and advantageous mutants.

Neutral mutants: First, we used the 2D agent-based model under the same assumptions as used in Fusco *et al.* (2016), *i.e.*, with neutral mutants and zero death rates ($L_w = L_m > 0$, $D_w = D_m = 0$). The same type of dynamics is observed as previously reported, with mutant clones either being engulfed by wild-type cells after creation, or mutant clones establishing growing sectors. The average number of mutants at size M is significantly larger for the spatial compared to the nonspatial system (data not shown).

Similar results are observed under the assumption that cells can die ($L_w = L_m > 0$, $D_w = D_m > 0$). Mutants either grow as expanding sectors or are engulfed by the wild-type cells after temporary expansion [Figure 1, inset in (A)]. The number of mutants at population size M is always larger in the spatial compared to the nonspatial system (Figure 1A). The extent of the difference is larger for higher death rates and lower reproduction rates, *i.e.*, for populations with a higher turnover (Figure 1A). This is because, in higher turnover systems, more generations are required to reach a given
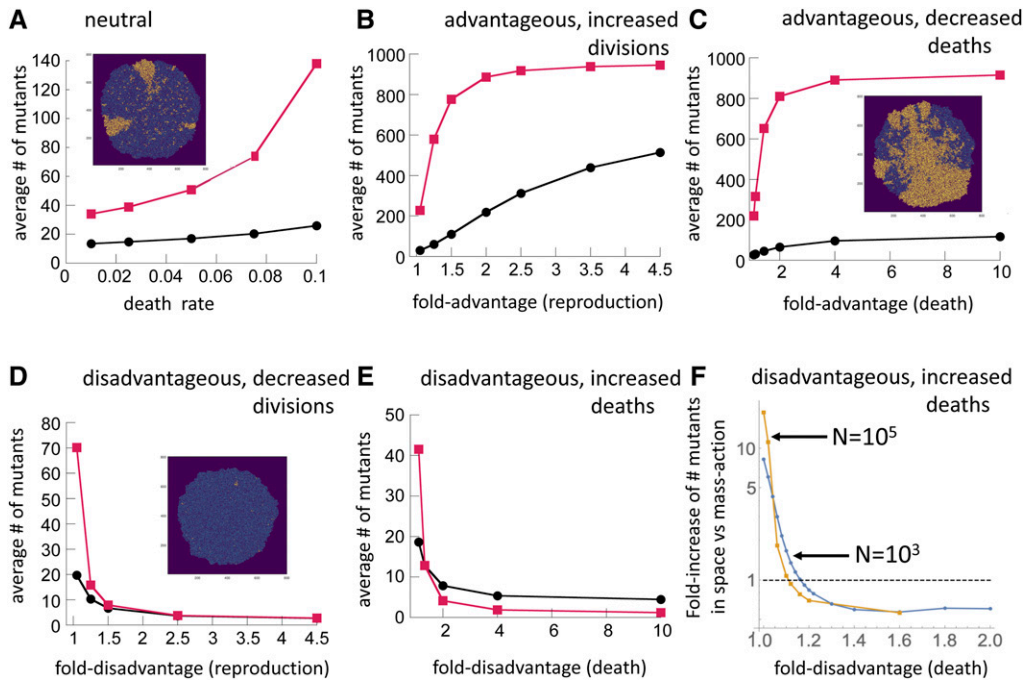
Figure 1 Comparison of the number of mutants in 2D spatial agent-based model simulations (red) and a well-mixed system (black). In (A–E), the lines represent the mean numbers of mutants in the spatial and nonspatial systems at equal size, $N = 10^3$. (A) Neutral mutants, as a function of the death rate. (B and C) Advantageous mutants, characterized by increased division rates (B) and decreased death rates (C), as a function of the fold-advantage. (D and E) Disadvantageous mutants characterized by decreased division rates (D) and increased death rates (E), as a function of the fold-disadvantage. Typical 2D spatial agent-based simulations of range expansion dynamics are shown in the insets for each mutant type. (F) The ratio of the mean number of mutants in the 2D spatial simulations and that for the well-mixed system, for disadvantageous mutants with increased death rates, is shown as a function of fold-disadvantage. The two lines correspond to population sizes of 10^3 (blue) and 10^5 (yellow). The parameters for (A–E) (unless otherwise indicated in figure) are: $L = 0.2$, $D = 0.1$, $u = 2 \times 10^{-3}$. For each parameter combination, from 2×10^6 to 3×10^7 repeats were performed; shown are the means; SE are too small to see. For (F), $L_w = L_m = 0.09$, $D_w = 0.05$, $u = 2 \times 10^{-3}$. SEs are represented by vertical bars and are not visible.

size threshold, resulting in the amplification of the observed effect.

Results of this comparison were qualitatively similar to those obtained from the patch model. The number of neutral mutants at population size M (assumed much smaller than the maximum system size) was always higher for the spatial (patch) compared to the well-mixed system (Supplemental Material, Figure S2A). Interestingly, this result holds for different spatial organizations of the patch model. In the most spatially restricted system, individuals can only migrate to and from the eight nearest neighboring patches. In an alternative model, migration is allowed between any patches regardless of their location. In either case, a patch model produces significantly more mutants than the mass-action system. This suggests that it is not the spatial arrangement *per se* but fragmentation of the system that may be responsible for the observed increased number of mutants. The difference is more pronounced for larger cell death rates (Figure S2A).

Advantageous mutants: If the mutant is advantageous, the dynamics are similar as those observed for neutral mutants. First, we assume that the advantage is given by a larger division rate of the mutant cells. The number of mutants at population size M is always larger in the spatial compared to the well-mixed setting (Figure 1, B and C); higher death rates lead to a larger difference between the number of mutants in spatial and nonspatial settings (Figure S1A in the Supplement). Mutants can again either grow as expanding sectors,

or show a temporary growth phase before being engulfed by wild-type cells, see inset in Figure 1C. Similar results are obtained if we assume that the mutant advantage is given through a reduced death rate of mutant cells (Figure 1Bii and Figure S1B in the Supplement). These conclusions remain robust if we use the patch model (either spatially constrained or with random migration between any two patches) instead of the agent-based model (Figure S2B of the Supplement). We note that the graphs cover a range of degrees to which the mutant is advantageous, starting from almost neutral up to a fourfold advantage (perhaps unrealistically high, where the spatial system is completely invaded by mutants). The aim was to show that results do not change for a large parameter range.

Disadvantageous mutants: Disadvantageous mutants are very unlikely to grow as sustained sectors, especially if the disadvantage is more pronounced (inset in Figure 1D). In the absence of death, after creation, mutants undergo a few cell divisions and are then engulfed by the expanding wild-type cell population; in the presence of cell death, they form mutant "islands," which can become repeatedly generated by mutations and tend to be outcompeted by wild-type cells.

The average number of mutants when the overall population reaches size M depends on spatial structure in a more complex way, compared to the case of neutral mutants. First, we assume that the fitness difference lies in the division rate of the cells (Figure 1D). In this case, we observe that the average

number of mutants is always larger for the spatial compared to the well-mixed simulations. The extent of the difference, however, becomes very small as the extent of the disadvantage grows. Hence, unless the mutant is almost neutral, the increase in the number of mutants in the spatial compared to the nonspatial system becomes negligible. In addition, the difference is most pronounced for small death rates and diminishes for larger death rates (Figure S1C of the Supplement).

A different result is observed if the lower fitness of the mutant strain is brought about by a higher death rate of mutant cells. If the difference in death rates lies above a threshold level, the average number of mutants at size M is observed to be larger in well-mixed compared to spatial simulations (Figure 1E), which is the opposite trend compared to the previous cases, and also the opposite result compared to those reported in Fusco *et al.* (2016). Figure 1F shows more details of this behavior. We observe that the number of mutants in a well-mixed system starts exceeding that of the spatial system when the % death rate increase is $\sim$16% for this parameter set (when measured at size 10^3), but this percentage decreases for larger population sizes: it is $\sim$12% when measured at size 10^5, and we expect that the effect is observed for even smaller degrees of disadvantage at larger sizes. This might be relevant for cancer cell populations, where the number of cells can reach 10^{10}–10^{13}. For smaller degrees of disadvantage, even though there are more mutants in the spatial system, the difference is drastically reduced compared to that reported for neutral systems (Figure 1F). This again indicates that a disadvantage in death counters the potential of spatial structure to increase mutant numbers. Lower reproduction rates result in more pronounced differences between the number of mutants in spatial and nonspatial settings (Figure S1D of the Supplement). All in all, the effect reported here is manifested for a wide range of disadvantages.

An analysis of the spatial stochastic model is developed in Section 3 of the Supplemental material. Using the pair approximation, we derive a formula for the selection-mutation balance of mutants away from the colony boundary (Eq. 36). This theory predicts patterns similar to those described above. An intuitive explanation of disadvantageous mutant behavior under decreased reproduction and increased death is provided in the next section, see Figure 3.

To confirm the robustness of these results, we performed simulations with disadvantageous mutants in a patch model. Again, the outcome of the dynamics depends on the parameters upon which the disadvantage is based, see Figure 2 for migration to nearest patches and Figure S12 for global migration. If the mutant has a lower division rate than the wild-type, the number of mutants at population size M is larger for the spatial than for the well-mixed scenario. This difference is largest if cells do not die, and diminishes with increasing cell death rates. If, however, the mutant is characterized by a larger death rate than the wild-type, then the opposite result is obtained: the number of mutants at population size M is smaller in the spatial than in the well-mixed system (as long as the difference in the death rate lies above a threshold). Again, the results are qualitatively similar for the spatially restricted (nearest neighbor) and nonrestricted (migration to all patches) models (see yellow symbols in the central panels of Figure 2 and Figure S12).

Deterministic (ODE) versions of the patch models are developed and analyzed in Section 2 of the Supplemental material; in particular, Section 2.5 provides approximate formulas for the numbers of mutants in a metapopulation model and shows for what division and death parameters the number of disadvantageous mutants is higher (lower) in the deterministic metapopulation model compared to the mass-action model. This confirms the above finding that, for mutants with lower division rates, more mutants occur in a deterministic metapopulation model, and for mutants with sufficiently high death rates, there are more mutants in mass-action.

Disadvantageous mutants: an intuitive explanation of growth patterns: An intuitive explanation of this phenomenon can be built by observing the growth patterns of disadvantageous mutants in a single patch, starting from a single wild-type cell (see Sections 2.5–2.6 of the Supplemental material for details). Typically, as the total population increases and reaches its carrying capacity, the mean number of mutants is an increasing function of the total population size, and it eventually on average saturates at the selection mutation balance. The number of mutants, however, does not grow proportional to the total population size; in fact, in some cases the percentage of mutants increases with size, and in others it decreases with size. It turns out that mutants characterized by decreased division rates, which grow relatively slowly at the initial stages, gradually increase in fraction and are most abundant at carrying capacity (Figure 3, blue line Figure 3A). On the other hand, mutants with larger death rates grow relatively fast at the initial stages (because they have the same division rates equal to those of the wild types, and initially behave like neutral mutants). As time goes by, however, the larger death rates of mutants start making a difference. The disadvantageous mutants start being "weeded out" and decrease in percentage down to the selection-mutation balance, when the system reaches carrying capacity (Figure 3, orange line in Figure 3A). In other words, if the mutants are characterized by decreased divisions, we expect to observe the largest fraction of mutants when the patch reaches its maximum population; in contrast, if the mutants are characterized by increased deaths, then the percentage of mutants is larger at intermediate stages of growth compared to patches that reach capacity.

Next, we note that a well-mixed system can be viewed as a superposition of identical, independent smaller patches that all grow simultaneously (Figure 3B). A (proper) patch model is also a collection of patches, but the growth in different patches does not happen simultaneously; instead, it starts in one patch, after a while a second patch starts growing,
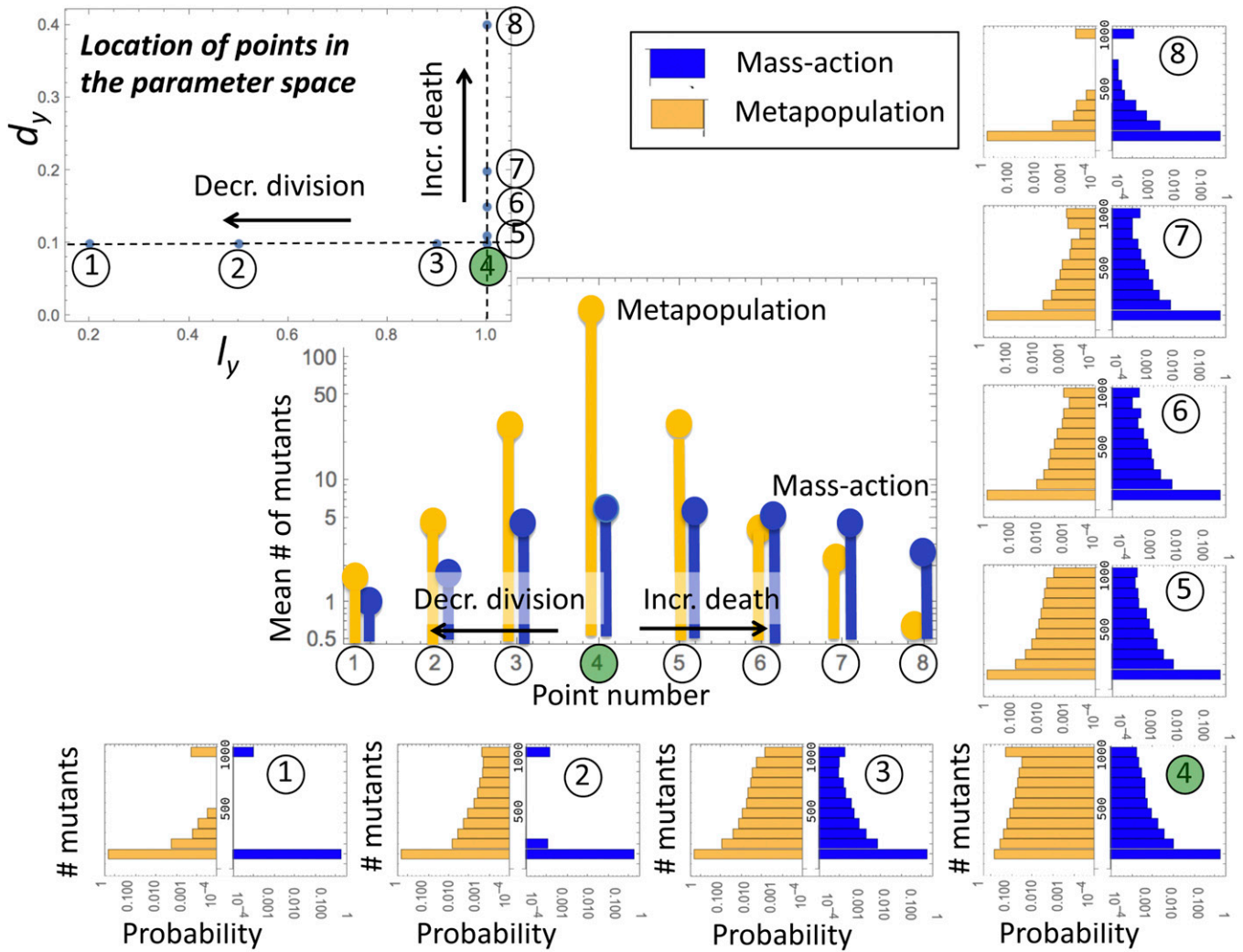
Figure 2 A systematic study of the number of disadvantageous mutants in mass-action (blue bars in histograms) and in patch model (yellow bars). Data are presented for eight parameter combinations: one to three with mutants of decreased division rates, four (the green point) with neutral mutants, and five to eight with mutants of increased death rate. We observe that the mean number of mutants in the patch models with nearest neighbor migrations (depicted by yellow symbols in the central panel) becomes smaller than that in the mass-action model (blue symbols) if the disadvantage through death is sufficiently large. The numerical probability distributions for the numbers of mutants are also presented for well-mixed and patch (with nearest neighbor migration) models; ~2 × 10⁵ simulations were used for each parameter combination. Please note the logarithmic scale of the histograms. The rest of the parameters are as follows: $u = 10^{-3}$, $m = 10^{-5}$, $k = 100$, 100 patches; the number of mutants evaluated at total population 10^3. See Figure S14 for the patch model with global migrations; the results are very similar.

etc. (Figure 3C). Therefore, an important difference between the well-mixed system and a patch system is that in the latter model, different patches are desynchronized, such that, at a given point in time, some patches are completely filled to capacity while others have not started growing yet.

Keeping this in mind, we can see whether a synchronized (well-mixed) or a desynchronized (patch) model will contain a larger number of mutants. If the mutants have decreased division rates and their percentage grows with total population size, then we are likely to find more mutants in a desynchronized system (spatial or fragmented) that consists of a number of full patches (maximum size, maximum mutant percentage), plus a number of empty patches that do not contribute. In a synchronized (*i.e.*, mixed) system, populations

in all patches will lie below carrying capacity at total size M, resulting in fewer mutants. On the other hand, if the mutants have increased death rates and their percentage is larger at the intermediate stages of population growth, then we expect to have more mutants in a fully synchronized system (*i.e.*, a mixed system), which is equivalent to a set of identical patches that are all relatively early in their growth and thus contain a relatively large percentage of mutants. In the desynchronized (spatial or fragmented) system, populations in several patches will have reached carrying capacity when the total population size reaches M, and thus will have already experienced a decline in mutant percentages.

Before we proceed, we would also like to address the topic of jackpot mutation events (Fusco *et al.* 2016). One can think
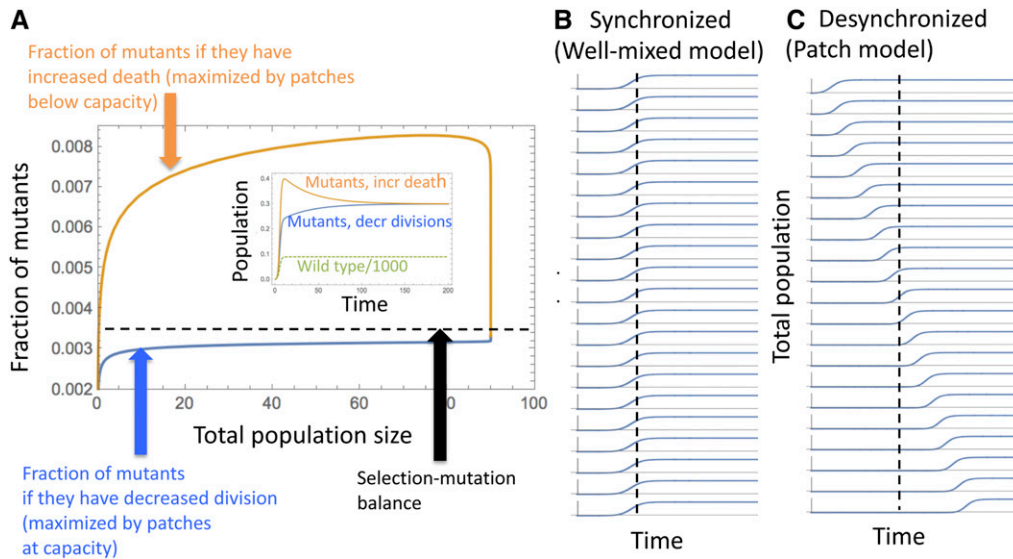
Figure 3 Disadvantageous mutants—an intuitive picture. (A) The fraction of mutants (characterized by increased death and by decreased divisions) as a function of the population size (ODEs, parameters as in Figure S5). Inset: the time-series for the mutant populations with increased (orange) and decreased (blue) death rates, together with the wild type population (scaled by 1000 to fit in the same graph). (B) A schematic representing total population time-series in different patches in a patch model. (C) Same for the well-mixed model represented as a collection of identical, synchronous patches. At the same total population size, in a patch model some populations are at carrying capacity, and some are zero, while in the well-mixed model, all the "patches" are partially filled. Patches with populations below carrying capacity have more mutants than patches at carrying capacity, if the mutants are characterized by increased death. Patches with populations below carrying capacity have fewer mutants than patches at carrying capacity, if the mutants are characterized by decreased divisions.

of those events as relatively long lineages of mutants that contribute significantly to the overall expected number of mutants in a growing colony. These lineages are more likely to grow in a spatial system, because a disproportionately large fraction of successful division events happens at the advancing front, thus resulting in the proliferation of individuals that are most separated from the founding individual, and which are more likely to have experienced a mutation. This argument certainly holds for neutral and advantageous mutants, but changes somewhat for disadvantageous mutants. First of all, jackpot events are less important in the latter case, because mutant clones are unlikely to expand and in any location, mutant levels eventually settle to a low percentage (dictated by selection-mutation balance). Further, if the disadvantage is manifested through an increase in death, relatively long mutant lineages that are more likely to pop up in spatial and fragmented systems, become progressively diminished by the process of weeding out the mutants, thus making the jackpot contributions smaller in spatial/fragmented systems compared to the mass-action case. This is explored numerically in section 3.5 of the Supplemental material.

Growth laws for neutral, advantageous, and disadvantageous mutants in spatial and nonspatial models

Observations presented so far can be generalized by deriving growth laws of mutants in different scenarios, see Table 1 and Section 4 of the Supplemental material for details.
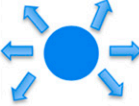
Consider the type of growth where the population spreads in one direction [examples of such growth can be found in the geometry of colonic crypts (Michor *et al.* 2004; Lopez-Garcia *et al.* 2010), or in mitotic zone germ cells in *Caenorhabditis*

elegans (Kershner *et al.* 2013)]. The mathematical abstraction of this process is the surface of a cylinder, which is a rectangular domain of width W, with the initial cell configuration aligned along one of the boundaries and periodic boundary conditions imposed in the transversal direction. The cell population in this case will engage in a linear growth, such that the mean total population N = W*L grows as N∼t. The number of disadvantageous mutants in this setting will scale with the total population as specified in the first column of Table 1 (2D flat), as these mutants will typically form finite "bubbles" and, thus, their number will be entirely driven by production. If mutants are neutral, then, on average, each newly created mutant will give rise to a clone that grows linearly in time, thus giving a quadratic growth law (uN^2), see Figure 4, curves (a,b). Finally, advantageous mutants, when created, will form expanding clones whose width will grow as the colony proceeds to expand; in other words, advantageous colonies comprise (on average) increasing fractions of the total population size, adding an extra power of N to the growth law (uN^3), see Figure 4, curves (c–g). In the case of a 2D flat front expansion, the number of neutral and advantageous mutants in a colony of a fixed size negatively correlates with the front width: the number of mutants is inversely proportion to the first power of width, W, for neutral, and to the second power of W for advantageous mutants, see Section 4.1 of the Supplemental material. Note that in the extreme case where $W = 1$, we have a one-dimensional (1D) growing array of cells. In this special case (Michor *et al.* 2004), in the absence of cell death, all mutants regardless of their fitness properties behave as uN^2.

Next, consider range expansion in 2D [*e.g.*, yeast colony expansion (Chen *et al.* 2014), 2D melanoma cultures (Qin *et al.* 2016; Cruz Rodríguez *et al.* 2019)], where the population

Table 1 The growth laws of mutants in different spatial and nonspatial growth scenarios, for disadvantageous, neutral, and advantageous scenarios. α is a parameter that quantifies the mutant advantage, $\alpha=(L_m-D_m)/(L_w-D_w)$

	2D flat	2D range	3D flat	3D range	Exponential
Mutant property					
Disadvantageous	uN	uN	uN	uN	uN
Neutral	uN^2	$uN^{3/2}$	uN^2	$uN^{4/3}$	$uN \ln N$
Advantageous	uN^3	uN^2	uN^4	uN^2	$uN^{(2\alpha-1)/\alpha}$

grows outward as an expanding circle. In this case, the total population follows the so-called surface growth: $N \sim t^2$. Mutant cells behave as specified in the second column of Table 1. In particular, disadvantageous mutants are again proportional to the total population; neutral mutations are expected to give rise to colonies whose size does not increase or decrease as a fraction of the total population (the 3/2 law), Figure 5, A and B; advantageous mutations create expanding colonies (the quadratic law), Figure 5, C–F. Note that our theoretical results for the advantageous mutants in a 2D range expansion confirm prior numerical results of Gralka and Hallatschek (2019).

In a 3D range expansion, which is relevant, for example, for most solid tumors or biofilms (Nadell *et al.* 2016), the total population engages in a 3D surface growth such that $N \sim t^3$. Mutants are predicted to behave as described in the fourth column of Table 1, and numerical examples confirming the predictions are presented in Figure 6. The 3D flat front expansion is described in the third column of Table 1, see also curves (d–f) of Figure 6. The growth of advantageous mutants in a colony with a 3D flat front is characterized by the highest power (the fourth power) of N. Further details are provided in Section 4.2 of the Supplemental material.

For comparison, results for nonspatial, exponential growth were derived, for example, by Iwasa *et al.* (2006) and are given in the last column of Table 1. The growth of advantageous mutants in an exponentially expanding population is given by M (exp, adv)$\sim uN^{(2\alpha-1)/\alpha}$, where α is a parameter that quantifies the mutant advantage ($\alpha = L_m - D_m)/(L_w - D_w)$). Note that as $\alpha \to \infty$, we have at most M(exp, adv)$\sim uN^2$, and for all finite values of fitness advantage, the power is <2.

These laws are valid under some restrictions specified in Section 4 of the Supplemental material. In particular, the laws for advantageous mutants hold for small mutant advantage,

and also on the time scales before all the cells in a growing colony's front are replaced by mutants. In the long term, the replacement of all cells by advantageous mutants is an inevitable outcome in the presence of death, and an approximate outcome as $t \to \infty$ even in the absence of death. Once this happens, the growth law will be M$\sim$N.

The laws of Table 1 are very general and hold in the presence and in the absence of cell death, and also in the presence and in the absence of back mutations (see *Materials and Methods*). The proportionality coefficients depend on particularities of the underlying dynamics (for example the type of grid used and the number of neighbors, as well as the death to division ratios), but the power laws are universal.

The growth laws derived here have direct consequences for the expected numbers of mutants in equally sized populations growing in different dimensions (and mass-action). The proportion of neutral mutants scales as uN for a flat front (in 2D or 3D), $uN^{1/2}$ for a 2D range expansion, $uN^{1/3}$ in a 3D range expansion, while it is $u \log N$ in exponentially growing populations (see also Fusco *et al.* 2016). That is, the number of neutral mutants is always larger in spatial systems compared to the well-mixed system. In space, the proportion of neutral mutants is the largest in low dimensions.

For advantageous mutants, the proportion of mutants is given by uN^3 for a 2D flat front and it is uN^4 for a flat front in 3D, while it is uN^2 for a range expansion (in 2D or 3D); it is $uN^{(\alpha-1)/\alpha}$ in exponentially growing populations. Again, it is the smallest in mass-action.

Finally, for disadvantageous mutants, the power law of mutant growth is the same in all dimensions (and is given by uN). Therefore the results are more subtle and depend on the particular setup. As was shown in the previous section, the behavior depends on whether the disadvantage is manifested through differences in division or death rates.
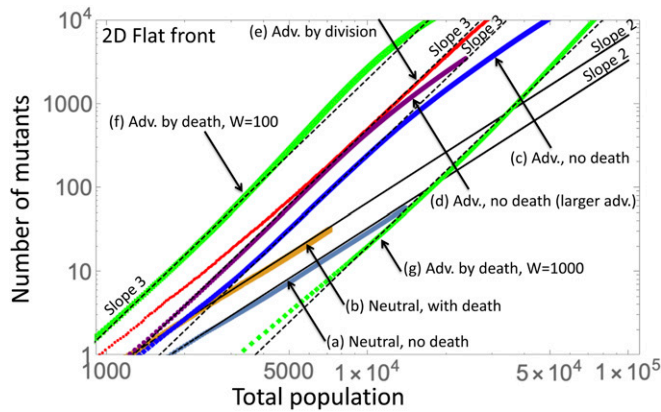
Figure 4 Mutants in a colony with a 2D flat front: the number of mutants as a function of the total population, averaged over 1000 stochastic runs (SE too small to see). Cases (A and B) are neutral, and the corresponding solid black lines are guides to the eye with slope 2 in the log–log plot. Cases (C and G) are advantageous, and the dashed lines are guides to the eye with slope 3. The following parameters are used: (A) Neutral, no death: $L_w = L_m = 0.7$, $D_w = D_m = 0$. (B) Neutral, with death: $L_w = L_m = 0.7$, $D_w = D_m = 0.2$. (C) Advantageous, no death: $L_w = 0.7$, $L_m = 0.9$, $D_w = D_m = 0$. (D) Advantageous, no death, larger advantage: $L_w = 0.7$, $L_m = 1.0$, $D_w = D_m = 0$. (E) Advantageous by division, with death: $L_w = 0.7$, $L_m = 0.8$, $D_w = D_m = 0.2$. (F) Advantageous by death: $L_w = L_m = 0.7$, $D_w = 0.2$, $D_m = 0.1$. (G) Same as (F), but with a wider front: $W = 1000$. The rest of the parameters are $u = 5 \times 10^{-5}$, $W = 100$ (except G).

Discussion

We have used computational models to study mutant evolution in spatially structured and fragmented populations, focusing on the average number of mutants present when the total population size has reached a threshold. Previous work, including Fusco *et al.* (2016), established that, for neutral mutants, spatial restriction results in a larger number of mutants that are present in a population of a defined size. This was attributed to jackpot events occurring even at relatively large population sizes in spatially structured populations due to the occurrence of range expansion. In contrast, jackpot mutation events can occur only at very early stages of growth in mixed systems. We extended this analysis by considering advantageous and deleterious mutants in greater detail, in the absence and presence of cell death, and assuming that mutant advantage/disadvantage was manifested through either the division or death rate. While the results for advantageous mutants were similar to those for neutral mutants (more mutants in spatial than mixed systems), we found a different trend for disadvantageous mutants. If disadvantage was mediated by an increase of the mutant death rate (rather than a decrease in the division rate), then the difference between the number of mutants in the spatial and well mixed systems becomes dramatically reduced, even for very slightly disadvantageous mutants, and, as the extent of the disadvantage crosses a threshold, the number of mutants in spatially structured populations becomes smaller than in mixed systems.
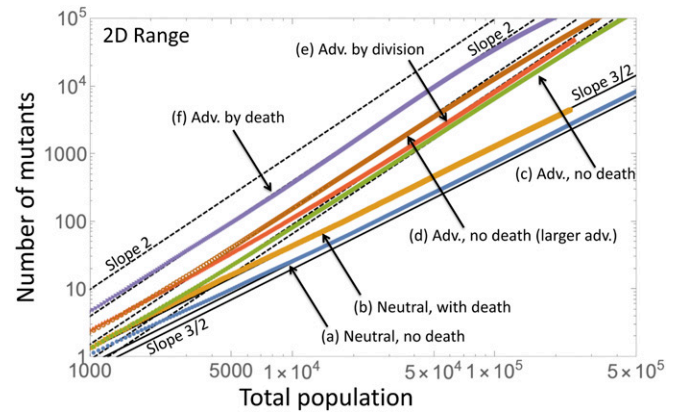
Figure 5 Mutants in the 2D range expansion: the average number of mutants as a function of the total population (SE too small to see). Cases (A and B) are neutral, and the corresponding solid black lines are guides to the eye with slope 3/2 in the log–log plot. Cases (C and F) are advantageous, and the dashed lines are guides to the eye with slope 2. The following parameters are used: (A) Neutral, no death: $L_w = L_m = 0.7$, $D_w = D_m = 0$, 2000 runs. (B) Neutral, with death: $L_w = L_m = 0.7$, $D_w = D_m = 0.2$, 1366 runs. (C) Advantageous, no death: $L_w = 0.7$, $L_m = 0.9$, $D_w = D_m = 0$, 2000 runs. (D) Advantageous, no death, larger advantage: $L_w = 0.7$, $L_m = 1.0$, $D_w = D_m = 0$, 2000 runs. (E) Advantageous by division, with death: $L_w = 0.7$, $L_m = 0.8$, $D_w = D_m = 0.2$, 1426 runs. (F) Advantageous by death: $L_w = L_m = 0.7$, $D_w = 0.2$, $D_m = 0.1$, 1396 runs. The mutation rate is $u = 5 \times 10^{-5}$.

The new insights about disadvantageous mutants have important practical implications, for example, for understanding the presence of drug resistant mutants prior to the start of treatment in cancers (Horswell *et al.* 2013) or bacterial populations that form a biofilm (Banin *et al.* 2017). According to our results, spatial structure can make it less likely that mutants are present before treatment is started, and, if they are present, their average numbers can be lower in spatially structured compared to mixed systems. This requires the disadvantage to be due to a larger death rate and the extent of the disadvantage to lie above a threshold. We have shown that the disadvantage threshold beyond which this effect is observed becomes lower with larger population sizes, indicating that this could be especially relevant for cancer and bacterial populations. Drug-resistant mutants have often been shown to be characterized by a fitness cost compared to drug-sensitive cells (Gagneux *et al.* 2006; Szakács *et al.* 2014), and this is well-documented in the literature for antibiotic resistance in bacteria (Andersson and Hughes 2010). The extent of the disadvantage varies depending on the bacterial infection in question, and on the setting in which bacterial growth is measured (Andersson and Hughes 2010). In a number of cases substantial fitness costs have been documented for drug-resistant bacteria (Wichelhaus *et al.* 2002; Yu *et al.* 2005; Nilsson *et al.* 2006; Andersson and Hughes 2010) (in the absence of compensatory mutations), *e.g.*, up to 40% fitness reduction in some rifampin-resistant *Staphylococcus aureus* populations (Wichelhaus *et al.* 2002), with even larger fitness costs reported in other studies (Andersson and Hughes 2010). The fitness cost of resistant mutants is likely
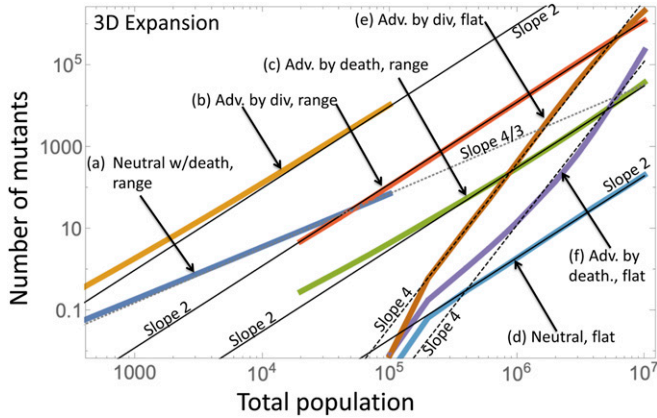
Figure 6 Mutants in the 3D expansion: the average number of mutants is plotted as a function of the total population. (A) Neutral mutants in a range expansion, with the corresponding dotted gray guide to the eye with slope 4/3 in the log–log plot. (B and C) Advantageous mutants in a range expansion, and the solid lines are guides to the eye with slope 2. (D) Neutral mutants in a 3D flat front expansion, and the solid guide to the eye has slope 2. (E and F) Advantageous mutants in a colony with a 3D flat expansion, the dashed guides to the eye have slope 4. The following parameters are used: (A) Neutral, range: $L_w = L_m = 0.7$, $D_w = D_m = 0.1$, $u = 2 \times 10^{-5}$, 10^7 runs. (B) Advantageous by division, range: yellow $L_w = 0.4$, $L_m = 0.8$, $D_w = D_m = 0.1$, $u = 2 \times 10^{-5}$, 4×10^6 runs; red same but $u = 2 \times 10^{-7}$, 66,631 runs. (C) Advantageous by death, range. (D) Neutral, flat: $L_w = L_m = 0.8$, $D_w = D_m = 0.1$, $u = 2 \times 10^{-7}$, 34,967 runs. (E) Advantageous by division, flat: $L_w = 0.4$, $L_m = 0.8$, $D_w = D_m = 0.1$, $u = 2 \times 10^{-7}$, 11,369 runs. (F) Advantageous by death, flat: $L_w = L_m = 0.7$, $D_w = 0.2$, $D_m = 0.1$, $u = 2 \times 10^{-7}$, 53,840 runs.

Table 2 Summary of the contributions of different mechanisms to mutant accumulation in expanding spatial/fragmented populations (see text)

Mutant type	(A)	(B)	(C)
Advantageous, no death	↓	↑	N/A
Advantageous, with death	↑	↑	N/A
Disadvantageous, no death	↑	↑	↑
Disadvantageous by divisions, with death	↓	↑	↑
Disadvantageous by death	↓	↑	↓

(A) is the role of fragmentation/spatial restrictions through changing selections strength, (B) is jackpot events, and (C) is the synchronization phenomenon. Here ↓ means "suppresses mutants in space, compared to exponential growth in well-mixed systems" and ↑ means "enhances mutants in space, compared to exponential growth in well-mixed systems."

to eventually become reduced or eliminated due to the acquisition of compensatory mutations (Gagneux *et al.* 2006), but the initial dynamics of mutant evolution before therapy will be significantly determined by the original fitness cost of the mutants. The results reported here about the effect of spatial structure on the evolution of disadvantageous mutations therefore provides valuable information to better understand the emergence of resistant strains before the onset of treatment, and thus for our ability to potentially predict treatment outcomes. This complements other work that has shown an important role of space for the dynamics of drug-resistant cells during therapy, through opening up space for the resistant mutants to grow through competitive release (Enderling *et al.* 2009; Hillen *et al.* 2013; Fusco *et al.* 2016).

Another interesting result was our finding that qualitatively similar results are obtained if we consider evolutionary dynamics in fragmented rather than spatially structured populations. The same outcomes were obtained for a patch model where individuals in each patch could migrate to any randomly chosen patch in the system (and not just the neighboring patches). Therefore, the properties of mutant evolution described here and also in Fusco *et al.* (2016) might not be a particular property of spatial systems, but more generally of fragmented systems. Our intuitive explanation for the differences in the numbers of disadvantageous mutants does not rely on any spatial restrictions in cell migration, but rather on

the desynchronization of mutant dynamics in the patches of a fragmented system.

In order to understand the intuitive reasons for the observed patterns, it is helpful to consider different ways in which space/fragmentation could influence the dynamics of mutants in expanding populations, see Table 2.

(A) How does space/fragmentation affect force of selection? While it is known in the literature that fragmentation may suppress selection (Wright 1931; Komarova 2006; Gralka and Hallatschek 2019), this notion has to be applied carefully in each situation. For example, in our setting, we are comparing an exponentially growing population where no selection at all takes place, to a spatially restricted or fragmented system, where in each patch or spatial location, individuals compete for space, thus leading to a suppression of weaker types and enhancement of stronger types. An exception is found in a patch model in the absence of death, see Section 1.2.2 of the Supplemental material.

(B) How do jackpot events influence mutant accumulation is space? Since in spatial and fragmented expanding systems, organisms that divide are more likely to be the ones that are further removed from the founding organisms (and thus are more likely to have acquired a mutation), jackpot events enhance mutant accumulation, although their role is stronger for advantageous than disadvantageous mutants.

(C) How does desynchronization experienced in spatial and fragmented systems affect the accumulation of mutants? This is something that we saw affecting disadvantageous mutants only, because the nature of the affect relies on convergence of the mutants toward selection-mutation balance. Mutants with lower division rates gain in relative abundance, while mutants with higher death rates lose in relative abundance (are weeded out), resulting, respectively, in their enhancement/suppression in spatial and fragmented settings compared to nonstructured systems.

Table 2 summarizes the three influences (A–C) listed here. We can see that, in the presence of death, there will always be

more advantageous mutants in space (and with no death, there are situations when we can find more in mass-action, Supplemental Section 1.2). For disadvantageous mutants, if they have increased death rates, there could be either more or fewer of them in space compared to well-mixed systems, as reported here. If they have decreased divisions, in the presence of death, this table shows that there could be some variable results, but we have not found a parameter regime with more such mutants in a well-mixed system (although the difference becomes vanishingly small for larger degrees of disadvantage.).

Our analysis of mutant evolution in expanding spatial populations led to a concise derivation of mutant growth laws (see Table 1) in systems of different dimensionalities and under different assumptions on mutant fitness. In particular, our formulas coincide with those previously derived for neutral mutants (Fusco *et al.* 2016) and confirm numerical predictions for advantageous mutants in 2D range expansions (Gralka and Hallatschek 2019).

Our work builds on and complements previous mathematical and computational investigations that explored the differences in mutant dynamics between spatial and nonspatial systems, such as the paper by Fusco *et al.* (2016). A variety of other papers dealt with related topics. For example, deleterious mutants were studied in by Lavrentovich *et al.* (2016) in the context of conversional meltdown, and it was shown that spatial settings enhance the spread and invasion of disadvantageous mutants. A study by Otwinowski and Krug (2014) analyzed the evolutionary dynamics characterized by a large and constant supply of beneficial or deleterious mutations in a 1D spatial habitat, by using the Wright–Fisher (constant population) dynamics. It was found that compared to nonspatial settings, selection is weakened, adaptation is slower, and fitness variation is larger. In paper by Gralka *et al.* 2016) it is shown that spatially structured populations with beneficial mutations can give rise to a higher mutant count than well-mixed populations, while in other scenarios (Gralka and Hallatschek 2019), fragmentation could reduce selection effects and lead to a lower mutant count. In general, our work fits into the larger literature concerned with spatial mutant evolution (Hallatschek 2018; Kayser *et al.* 2019; Paulose *et al.* 2019; Paulose and Hallatschek 2020) and structured populations (Frean *et al.* 2013; Hindersin *et al.* 2016; Allen *et al.* 2017; Giaimo *et al.* 2018).

To conclude, this study has demonstrated complex evolutionary dynamics in populations that are not well-mixed. We demonstrated that evolution can be influenced in different ways by spatial structure or habitat fragmentation, depending on the relative fitness of the mutant and depending on the parameter through which the fitness difference is expressed. These results can also guide future experiments to address some of the computational observations reported here. Experimental results from 2D spatial growth of cells, such as reported in Fusco *et al.* (2016), should be compared to analogous results from a fragmented system, for example where cells are grown in a collection of different wells and periodically transferred to other, randomly chosen wells. This could test our prediction that the mutant growth in the two scenarios follows similar patterns. On a more complex level, it would be interesting to devise an experimental system where the evolutionary dynamics of disadvantageous mutants is studied, comparing scenarios where the disadvantage is brought about by a difference in cell death *vs.* cell division.

Acknowledgments

Literature Cited

Allen, B., G. Lippner, Y.-T. Chen, B. Fotouhi, N. Momeni *et al.*, 2017 Evolutionary dynamics on any population structure. Nature 544: 227–230. https://doi.org/10.1038/nature21723

Andersson, D. I., and D. Hughes, 2010 Antibiotic resistance and its cost: is it possible to reverse resistance? Nat. Rev. Microbiol. 8: 260–271. https://doi.org/10.1038/nrmicro2319

Banin, E., D. Hughes, and O. P. Kuipers, 2017 Editorial: bacterial pathogens, antibiotics and antibiotic resistance. FEMS Microbiol. Rev. 41: 450–452. https://doi.org/10.1093/femsre/fux016

Block, M., E. Scholl, and D. Drasdo, 2007 Classifying the expansion kinetics and critical surface dynamics of growing cell populations. Phys. Rev. Lett. 99: 248101. https://doi.org/10.1103/PhysRevLett.99.248101

Brú, A., S. Albertos, J. Luis Subiza, J. L. Garcia-Asenjo, and I. Bru, 2003 The universal dynamics of tumor growth. Biophys. J. 85: 2948–2961. https://doi.org/10.1016/S0006-3495(03)74715-8

Brú, A., J. M. Pastor, I. Fernaud, I. Bru, S. Melle *et al.*, 1998 Super-rough dynamics on tumor growth. Phys. Rev. Lett. 81: 4008–4011. https://doi.org/10.1103/PhysRevLett.81.4008

Chen, L., J. Noorbakhsh, R. M. Adams, J. Samaniego-Evans, G. Agollah *et al.*, 2014 Two-dimensionality of yeast colony expansion accompanied by pattern formation. PLoS Comput. Biol. 10: e1003979. https://doi.org/10.1371/journal.pcbi.1003979

Coldman A. J. and J. H. Goldie, 1983 A model for the resistance of tumor cells to cancer chemotherapeutic agents. Math. Biosci. 65: 291–307. https://doi.org/10.1016/0025-5564(83)90066-4

Dewanji, A., E. G. Luebeck, and S. H. Moolgavkar, 2005 A generalized Luria-Delbruck model. Math. Biosci. 197: 140–152. https://doi.org/10.1016/j.mbs.2005.07.003

Enderling, H., A. R. Anderson, M. A. Chaplain, A. Beheshti, L. Hlatky *et al.*, 2009 Paradoxical dependencies of tumor dormancy and progression on basic cell kinetics. Cancer Res. 69: 8814–8821. https://doi.org/10.1158/0008-5472.CAN-09-2115

Frean, M., P. B. Rainey, and A. Traulsen, 2013 The effect of population structure on the rate of evolution. Proc. Biol. Sci. 280: 20130211. https://doi.org/10.1098/rspb.2013.0211

Freyer, J. P., and R. M. Sutherland, 1985 A reduction in the in situ rates of oxygen and glucose consumption of cells in EMT6/Ro spheroids during growth. J. Cell. Physiol. 124: 516–524. https://doi.org/10.1002/jcp.1041240323

Fusco, D., M. Gralka, J. Kayser, A. Anderson, and O. Hallatschek, 2016 Excess of mutational jackpot events in expanding populations revealed by spatial Luria-Delbruck experiments. Nat. Commun. 7: 12760. https://doi.org/10.1038/ncomms12760

Gagneux, S., C. D. Long, P. M. Small, T. Van, G. K. Schoolnik *et al.*, 2006 The competitive cost of antibiotic resistance in Mycobacterium tuberculosis. Science 312: 1944–1946. https://doi.org/10.1126/science.1124410

Giaimo, S., J. Arranz, and A. Traulsen, 2018   Invasion and effective size of graph-structured populations. PLoS Comput. Biol. 14: e1006559. https://doi.org/10.1371/journal.pcbi.1006559

Gillespie, D. T., 1977   Exact stochastic simulation of coupled chemical-reactions. J. Phys. Chem. 81: 2340–2361. https://doi.org/10.1021/j100540a008

Goldie, J. H., and A. J. Coldman, 1998   *Drug Resistance in Cancer: Mechanisms and Models*. Cambridge University Press, Cambridge, UK. https://doi.org/10.1017/CBO9780511666544

Gralka, M., and O. Hallatschek, 2019   Environmental heterogeneity can tip the population genetics of range expansions. eLife 8: e44359. https://doi.org/10.7554/eLife.44359

Gralka, M., F. Stiewe, F. Farrell, W. Mobius, B. Waclaw *et al.*, 2016   Allele surfing promotes microbial adaptation from standing variation. Ecol. Lett. 19: 889–898. https://doi.org/10.1111/ele.12625

Günther, S., C. Ruhe, M. G. Derikito, G. Bose, H. Sauer *et al.*, 2007   Polyphenols prevent cell shedding from mouse mammary cancer spheroids and inhibit cancer cell invasion in confrontation cultures derived from embryonic stem cells. Cancer Lett. 250: 25–35. https://doi.org/10.1016/j.canlet.2006.09.014

Hallatschek, O., 2018   Selection-like biases emerge in population models with recurrent jackpot events. Genetics 210: 1053–1073. https://doi.org/10.1534/genetics.118.301516

Hillen, T., H. Enderling, and P. Hahnfeldt, 2013   The tumor growth paradox and immune system-mediated selection for cancer stem cells. Bull. Math. Biol. 75: 161–184. https://doi.org/10.1007/s11538-012-9798-x

Hindersin, L., B. Werner, D. Dingli, and A. Traulsen, 2016   Should tissue structure suppress or amplify selection to minimize cancer risk? Biol. Direct 11: 41. https://doi.org/10.1186/s13062-016-0140-7

Horswell, S., N. Matthews, and C. Swanton, 2013   Cancer heterogeneity and "the struggle for existence": diagnostic and analytical challenges. Cancer Lett. 340: 220–226. https://doi.org/10.1016/j.canlet.2012.10.031

Iwasa, Y., M. A. Nowak, and F. Michor, 2006   Evolution of resistance during clonal expansion. Genetics 172: 2557–2566. https://doi.org/10.1534/genetics.105.049791

Johnson, P. J., and B. R. Levin, 2013   Pharmacodynamics, population dynamics, and the evolution of persistence in Staphylococcus aureus. PLoS Genet. 9: e1003123. https://doi.org/10.1371/journal.pgen.1003123

Kayser, J., C. F. Schreck, M. Gralka, D. Fusco, and O. Hallatschek, 2019   Collective motion conceals fitness differences in crowded cellular populations. Nat. Ecol. Evol. 3: 125–134. https://doi.org/10.1038/s41559-018-0734-9

Kepler, T. B., and M. Oprea, 2001   Improved inference of mutation rates: I. An integral representation for the Luria–Delbrück distribution. Theor. Popul. Biol. 59: 41–48. https://doi.org/10.1006/tpbi.2000.1498

Kershner, A., S. L. Crittenden, K. Friend, E. B. Sorensen, D. F. Porter *et al.*, 2013   Germline stem cells and their regulation in the nematode Caenorhabditis elegans. Adv. Exp. Med. Biol. 786: 29–46. https://doi.org/10.1007/978-94-007-6621-1_3

Kimura, M., 1962   On the probability of fixation of mutant genes in a population. Genetics 47: 713–719.

Komarova, N. L., 2006   Spatial stochastic models for cancer initiation and progression. Bull. Math. Biol. 68: 1573–1599. https://doi.org/10.1007/s11538-005-9046-8

Komarova, N. L., and D. Wodarz, 2010   ODE models for oncolytic virus dynamics. J. Theor. Biol. 263: 530–543. https://doi.org/10.1016/j.jtbi.2010.01.009

Komarova, N. L., and D. Wodarz, 2005   Drug resistance in cancer: principles of emergence and prevention. Proc. Natl. Acad. Sci. USA 102: 9714–9719. https://doi.org/10.1073/pnas.0501870102

Komarova, N. L., L. Wu, and P. Baldi, 2007   The fixed-size Luria–Delbrück model with a nonzero death rate. Math. Biosci. 210: 253–290. https://doi.org/10.1016/j.mbs.2007.04.007

Lavrentovich, M. O., M. E. Wahl, D. R. Nelson, and A. W. Murray, 2016   Spatially constrained growth enhances conversional meltdown. Biophys. J. 110: 2800–2808. https://doi.org/10.1016/j.bpj.2016.05.024

Lopez-Garcia, C., A. M. Klein, B. D. Simons, and D. J. Winton, 2010   Intestinal stem cell replacement follows a pattern of neutral drift. Science 330: 822–825. https://doi.org/10.1126/science.1196236

Luria, S. E., and M. Delbruck, 1943   Mutations of bacteria from virus sensitivity to virus resistance. Genetics 28: 491–511.

Michor, F., Y. Iwasa, H. Rajagopalan, C. Lengauer, and M. A. Nowak, 2004   Linear model of colon cancer initiation. Cell Cycle 3: 358–362. https://doi.org/10.4161/cc.3.3.690

Murphy, H., H. Jaafari, and H. M. Dobrovolny, 2016   Differences in predictions of ODE models of tumor growth: a cautionary example. BMC Cancer 16: 163. https://doi.org/10.1186/s12885-016-2164-x

Nadell, C. D., K. Drescher, and K. R. Foster, 2016   Spatial structure, cooperation and competition in biofilms. Nat. Rev. Microbiol. 14: 589–600. https://doi.org/10.1038/nrmicro.2016.84

Nilsson, A. I., A. Zorzet, A. Kanth, S. Dahlstrom, O. G. Berg *et al.*, 2006   Reducing the fitness cost of antibiotic resistance by amplification of initiator tRNA genes. Proc. Natl. Acad. Sci. USA 103: 6976–6981. https://doi.org/10.1073/pnas.0602171103

Otwinowski, J., and J. Krug, 2014   Clonal interference and Muller's ratchet in spatial habitats. Phys. Biol. 11: 056003. https://doi.org/10.1088/1478-3975/11/5/056003

Patwa, Z., and L. M. Wahl, 2008   The fixation probability of beneficial mutations. J. R. Soc. Interface 5: 1279–1289. https://doi.org/10.1098/rsif.2008.0248

Paulose, J., and O. Hallatschek, 2020   The impact of long-range dispersal on gene surfing. Proc. Natl. Acad. Sci. USA 117: 7584–7593. https://doi.org/10.1073/pnas.1919485117

Paulose, J., J. Hermisson, and O. Hallatschek, 2019   Spatial soft sweeps: patterns of adaptation in populations with long-range dispersal. PLoS Genet. 15: e1007936. https://doi.org/10.1371/journal.pgen.1007936

Qin, Y., J. Roszik, C. Chattopadhyay, Y. Hashimoto, C. Liu *et al.*, 2016   Hypoxia-driven mechanism of vemurafenib resistance in melanoma. Mol. Cancer Ther. 15: 2442–2454. https://doi.org/10.1158/1535-7163.MCT-15-0963

Rodriguez-Brenes, I. A., N. L. Komarova, and D. Wodarz, 2013   Tumor growth dynamics: insights into evolutionary processes. Trends Ecol. Evol. 28: 597–604. https://doi.org/10.1016/j.tree.2013.05.020

Cruz Rodríguez, N. C., J. Lineros, C. S. Rodríguez, L. M. Martínez, and J. A. Rodríguez, 2019   Establishment of two dimensional (2D) and three-dimensional (3D) melanoma primary cultures as a tool for in vitro drug resistance studies, pp. 119–131 in *Immune Checkpoint Blockade*, edited by Y. Pico de Coaña. Humana Press, New York, NY. https://doi.org/10.1007/978-1-4939-8979-9_8

Szakács, G., M. D. Hall, M. M. Gottesman, A. Boumendjel, R. Kachadourian *et al.*, 2014   Targeting the Achilles heel of multidrug-resistant cancer by exploiting the fitness cost of resistance. Chem. Rev. 114: 5753–5774. https://doi.org/10.1021/cr4006236

Talkington, A., and R. Durrett, 2015   Estimating tumor growth rates in vivo. Bull. Math. Biol. 77: 1934–1954. https://doi.org/10.1007/s11538-015-0110-8

Waclaw, B., I. Bozic, M. E. Pittman, R. H. Hruban, B. Vogelstein *et al.*, 2015   A spatial model predicts that dispersal and cell turnover limit intratumour heterogeneity. Nature 525: 261–264. https://doi.org/10.1038/nature14971

Wichelhaus, T. A., B. Boddinghaus, S. Besier, V. Schafer, V. Brade *et al.*, 2002 Biological cost of rifampin resistance from the perspective of Staphylococcus aureus. Antimicrob. Agents Chemother. 46: 3381–3385. https://doi.org/10.1128/AAC.46.11.3381-3385.2002

Wright, S., 1931 Evolution in Mendelian populations. Genetics 16: 97.

Yu, J., J. Wu, K. P. Francis, T. F. Purchio, and J. L. Kadurugamuwa, 2005 Monitoring in vivo fitness of rifampicin-resistant Staphylococcus aureus mutants in a mouse biofilm infection model. J. Antimicrob. Chemother. 55: 528–534. https://doi.org/10.1093/jac/dki053

Zheng, Q., 1999 Progress of a half century in the study of the Luria-Delbruck distribution. Math. Biosci. 162: 1–32. https://doi.org/10.1016/S0025-5564(99)00045-0

Communicating editor: L. Wahl